Neonatal Nicotine Exposure Primes Midbrain Neurons to a Dopaminergic Phenotype and Increases Adult Drug Consumption

Supplemental Information

SUPPLEMENTARY METHODS AND MATERIALS

Animals

Male and female C57BL/6J, VGAT-Cre (Slc32a1$^{tm2(cre)Lowl}$/J) and VGLUT2-Cre (Slc17a6 $^{tm2(cre)Lowl}$/J) were housed on a 12 h/12 h light/dark cycle in groups of 2-5 in a humidity- and temperature-controlled animal facility with free access to food and water. Male and female C57BL/6J mice from mothers implanted with either saline- or nicotine-loaded osmotic minipumps were used for the nicotine preference test, immunohistochemistry, calcium imaging and pan-neuronal DREADD-induced activity manipulation experiments. Male and female VGAT-Cre (Slc32a1$^{tm2(cre)Lowl}$/J) and VGLUT2-Cre (Slc17a6 $^{tm2(cre)Lowl}$/J) mice from mothers implanted with either saline- or nicotine-loaded osmotic minipumps were used for Cre-dependent DREADDs-induced neuronal excitation and selective Nurr1 downregulation experiments. All the experiments were conducted in accordance with the guidelines of the American Association for the Accreditation of Laboratory Animal Care and National Research Council's Guide for the Care and Use of Laboratory Animals and approved by the University of California San Diego Institutional Animal Care and Use Committee.

Neonatal nicotine exposure

Neonatal mice were exposed to 2 mg/Kg/day nicotine from P2 to P16 through lactation. Females with P2 litters were anesthetized with a Ketamine/Xilazine cocktail (10 mg/Kg)

and an osmotic minipump (ALZET, mod. 2002) delivering 2 mg/Kg/day nicotine (base) or sterile saline was implanted subcutaneously. Nicotine and cotinine presence in mothers and pups' blood were confirmed through HPLC (NMS Labs) (Fig. S1).

Immunocytochemistry

Free-floating DAB and fluorescent immunocytochemistry (IHC) were performed as described in Dulcis et al., 2013 (1). Deeply anesthetized (Ketamine/Xilazine, 10 mg/Kg) animals were intracardially perfused with PBS solution followed by 50 mL 4% PFA. Frozen brains were sectioned (30 µm) with a standard Leica Microtome (SM 2010R). Immuno-fluorescence protocols (2) were performed to identify VTA neurons with markers for TH (1:500, Millipore), Nurr1 (1:300, Santa Cruz), GFP (1:1000, Millipore), cFos (1:200, Santa Cruz). Fluorescent-tagged secondary antibodies (AlexaFluor anti-mouse 488/647 nm, anti-rabbit 488/555/594 nm, anti-goat 488/555 nm, and anti-chicken 488 nm) were all used at a 1:300 dilution ratio. For DAB IHC, 30 µm sections were mounted in gelatin on glass slides, coverslipped with Cytoseal mounting media (Thermo Scientific).

RNAscope in-situ hybridization

RNAscope in-situ hybridization (ACDbio) for TH, Nurr1, α4, VGAT and VGLUT2 mRNA was performed following manufacturer instructions. Mice were anesthetized with a Ketamine/Xilazine cocktail (10 mg/Kg), then brain was rapidly harvested and snap-frozen with powdered dry ice and 20 μm sections collected with a cryostat (Leica). Fluorescent images of 8 VTA sections/group were acquired with a confocal microscope (Leica SPe)

and cells showing 3 or more mRNA puncta were counted as positive by a user blind to experimental groups.

qRT-PCR

Quantitative RT-PCR was used to measure nAChRs RNA expression levels as described in Lippi et al., 2016 (3). Mice were deeply anesthetized (Ketamine/Xilazine, 10 mg/Kg), then decapitated, and the brains were dissected on an ice pad in RNAse free condition. The VTA was isolated and stored in 0.5 mL RNA-Later (Quiagen) at -40°C. RNA extraction was performed with a Quiagen RNAeasy mini-kit according to manufacturer's instructions and tested for purity and integrity. Total RNA was reverse transcribed by random decamer primer protocol (RETROscript kit, Ambion) according to manufacturer's instructions. TAQman Real-Time PCR analysis was conducted on a Light Cycler 480 system (Roche), and the data were processed and analyzed using the comparative Δ_{CT} method. nAChRs primers (Integrated DNA Technologies) were designed using the Roche online tool (Assay Design Center) and validated before use.

Quantification of DA and DA metabolites

AN-exposed NS and NN mice were rapidly decapitated and brains were quickly harvested. NAc was dissected bilaterally on an ice pad, immediately frozen on powdered dry ice and stored at -80C. Samples were analyzed at Vanderbilt Neurochemical Core by HPLC.

Viral injections into the VTA

Mice were anesthetized with 3% isoflurane and placed in a stereotaxic apparatus (RWD, mod. 68001) with a continuous flow of 1% isoflurane. Posterior VTA was targeted according to atlas coordinates (Paxinos) and previous experience (AP -3.0, L ±0.3, DV -4.6). 400 nL ($2.1x10^{13}$ GC/mL) of AAV1.Syn.GCaMP6f.WPRE.SV40 (Penn Vector Core) or AAV5.Syn.FLEX.GCaMP6f.WPRE.SV40 (AddGene) at 100 nL/min ratio were injected for calcium imaging experiments. AAV5.hSyn.DIO.hM3Dq.mCherry (AddGene, 300 nL, $1.3x10^{13}$ GC/mL) was injected at 100 nL/min ratio for DREADD-induced hyperactivity experiments. AAV5.hSyn.hM4D(Gi).mCherry (AddGene, 2 x 200 nL, $4.9x10^{12}$ GC/mL) was injected bilaterally at 100 nL/min ratio for pan-neuronal DREADD-induced inhibition experiments. AAVdj.DIO.eGFP (Salk Institute, 300 nL, $4.9x10^{12}$ GC/mL) was injected at 100 nL/min ratio for VGAT-Cre and VGLUT2-Cre cells tracing experiments. Either AAV5.TRMS.Nurr1 (300 nL, $1.0x10^{13}$ GC/mL) or AAV5.TRMS.GFP (300 nL $1.6x10^{13}$ GC/mL) were injected at 100 nL/min ratio for Nurr1 overexpression experiments. CRE-dependent miRNA viral genomes were engineered based on the same principle as DIO vectors. However, in order to prevent antisense transcription of the miRNA in this construct the promoter was situated within the lox sites (4). 2 x 200 nL ($2.0x10^{13}$ GC/mL) of the resultant vectors (AAV5.DIO.FmiR.Nurr1.GFP or AAV5.DIO.FmiR.SCR.GFP) was injected bilaterally at 100 nL/min ratio for selective downregulation of Nurr1 experiments. In house AAVs were produced as previously described (5). Validation images of site of injections for different construct are provided in Fig. S8.

Retrograde tracing

Stereotaxic injections of fluorescent RetroBeads (LumaFluor, Inc.) in the NAc medial shell (AP -1.78, L ±0.5, DV -4.1) were performed as described for viral injections. 80 nL of fluorescent RetroBeads were unilaterally injected in the NAc medial shell of P80 mice (Fig. S8). Mice were sacrificed at P90 after 10 days of recovery to allow adequate time for retrograde transport of RetroBeads from the NAc terminals to the soma of VTA neurons. RetroBead-labeled cell bodies in the VTA were imaged with confocal microscope (Leica SPe).

Calcium imaging

Calcium Imaging on ex-vivo brain slices was performed as described in Ting et al., 2014 (6). P90 NS- and NN-exposed mice previously injected (at P75) with AAV expressing GCaMP6f (Fig. S8) were deeply anesthetized with Ketamine/Xilazine, 10 mg/Kg and perfused intracardially with 20 mL of ice-cold NMDG-ACSF (92 mM NMDG, 2.5 mM KCl, 1.25 mM NaH_2PO_4, 30 mM $NaHCO_3$, 20 mM HEPES, 25 mM glucose, 2 mM thiourea, 5 mM sodium ascorbate, 3 mM sodium pyruvate, 0.5 mM $CaCl_2$, 10 mM $MgSO_4$). Dissected brains were glued onto a 4% agarose block for vibratome (Leica, VT100P) sectioning. The sample chamber was filled with ice-cold, continuously carbonated (95% O_2 - 5% CO_2) NMDG-ACSF. VTA-containing 300 µm-thick sections were kept at 34°C for 10 min to recover, then carefully transferred to a continuously carbonated HEPES-ACSF holding solution (92 mM NaCl, 2.5 mM KCl, 1.25 mM NaH_2PO_4, 30 mM $NaHCO_3$, 20 mM HEPES, 25 mM glucose, 2 mM thiourea, 5 mM sodium ascorbate, 3 mM sodium pyruvate, 2 mM $CaCl_2$, 2 mM $MgSO_4$) for at least 1 hour at room temperature before imaging. Live imaging

(2-Hz acquisition rate) of calcium spikes was obtained with confocal microscope (Leica SPe). Brain sections were placed in the imaging chamber with a Pasteur pipette and perfused continuously with a constant flow of ACSF recording solution (119 mM NaCl, 2.5 mM KCl, 1.25 mM NaH_2PO_4, 24 mM $NaHCO_3$, 12.5 mM glucose, 2 mM $CaCl_2$, 2 mM $MgSO_4$) at 37°C. Nicotine (1μM, base) were added to the recording ACSF for nicotine stimulation. Each VTA section was recorded for 10 minutes while perfusing with ACSF, then for 5 minutes while perfusing with 1 μM nicotine and then another 10 minutes of washout with regular ACSF. At the end of each recording session, slices were perfused with 1mM KCl to elicit maximum calcium response from all neurons (Video S1). Videos were analyzed with the MATLAB (Mathworks) software customized to measure calcium-spike number, frequency and duration as described in Lippi et al., 2017 (3).

Chronic chemogenetic activation/inhibition of non-DAergic VTA neuronal populations

P75 mice were injected (Fig. S8) with AAV expressing different DREADD constructs and housed for 2 weeks to allow sufficient overexpression post-transduction. DREADD ligand clozapine (CLZ) (7) was chronically injected (0.01 mg/Kg) twice a day for 2 weeks (P90 – P105) in NS- and NN-exposed VGLUT2-Cre and VGAT-Cre mice. At the end of the treatment, mice were tested in the open field paradigm, then sacrificed and their brains processed for immunohistochemistry.

Nicotine/ethanol preference test

Nicotine/Ethanol 2 bottle-choice test was performed on single-housed adult NS- and NN-treated mice as described in Meliska et al., 1995 (8). Mice were housed in standard cages with one bottle filled with water and the second with a nicotine or ethanol solution. Several nicotine concentrations (50 mg/L, 75 mg/L, and 100 mg/L of nicotine tartrate) and 6% ethanol solution were tested. Nicotine, ethanol, and water consumption were measured by weighing the bottles every week to monitor consumption over time. Bottles sides were switched weekly to avoid side biased preference. Δ nicotine/water ratio was defined by the % of change in nicotine preference between the first and last week of experiment. Animals were then sacrificed (P120) and their brains processed for immunohistochemistry.

Quinine taste discrimination test

Quinine taste discrimination was performed on single-housed adult (P90) NS- and NN-treated mice. A concentration of 2mM quinine hemisulfate (MP Biomedical) was tested. Quinine and water consumption were measured by weighing the bottles every week for 4 weeks to monitor consumption over time. Bottles sides were switched weekly to avoid side biased preference. Target Power value=0.8, Alpha level=0.05, estimate of effect size d=2.0, N=6/group.

Progressive ratio

Food-deprived mice were trained to press a lever in an operant chamber to get a reward (food pellet) on a fixed ratio 1 (FR1) schedule until they received 50 rewards for 3

consecutive days and for 3 more days in a FR5 schedule. Once the training phase was complete, mice underwent a 120 min PRB test for 3 consecutive days: mice had to press the lever an increasing number of times in order to get the reward. Sample sizes estimate based on the effect size of preliminary experiments (Power=0.78, Alpha=0.05, Cohen's d=2.1, N=6). Target Power value=0.8, Alpha level=0.05, estimate of effect size d=2.0, N=6/group.

Open field test

Animals were brought into the experimental room 1h prior testing to allow habituation. Mice were placed in the center of a 1m x 1m open field arena (SD instrument) and allowed to freely explore for 10 min; then they were challenged with a single injection of 0.01 mg/Kg clozapine or vehicle and allowed to freely explore the arena for 10 more minutes. Locomotor activity and time spent in center vs periphery was recorded with infrared beams connected to a tracing software (SD instrument).

Stereological quantitation of neuronal subtypes

Unbiased stereological counts of DAB-stained neurons were obtained with a Leica DM4 B equipped with Stereologer2000 software by user blind to experimental groups. Fluorescent images were acquired with a confocal microscope (Leica SPe) and cells were counted by a user blind to experimental groups with Adobe Photoshop built-in counting tool. An exhaustive count of TH-immunostained neurons (Slab Sampling Interval: 1; Total Number of Sections: 10; Section Sampling Interval: 1) was performed with a 63X oil objective on VTA coronal sections starting from Bregma -3.27 (AP). TH-immunostained

neurons were counted using a total of 100 dissectors (Frame Area: 5000 μm^2, Frame Height: 30 µm, Guard Height: 2 µm, Frame Spacing: 120 µm) per sub-nucleus per animal. A neuron was considered positive when its nucleus fell inside the dissector borders not touching the exclusion lines. Maximized fluorescence final images were obtained from a total of 17 Z-stacked layers 1.5 µm far from each other. For multiple fluorescence images, each channel was acquired individually with the same parameters described before, and final merged images were reconstructed with Adobe Photoshop. Various marker-stained neurons were quantified on a total of 5 (1 every 3) coronal VTA sections starting from Bregma -3.27 (AP). Nuclei were counterstained with DRAQ5 (1µL/mL, BioStatus).

Statistical analysis

Normally distributed data were analyzed using two-tailed Student's t-test (with Welch's correction when required) and one-way, two-way or repeated measures ANOVA, followed by appropriate post-hoc comparison. Non-normally distributed data were analyzed using Mann-Whitney U test and Kolmogorov-Smirnov test. Extreme outliers were identified using ROUT method with Q=0.1% and excluded from analysis. Alpha level was set to 0.05. Appropriate sample size for each experiment have been determined with standard Cohen's d power analysis with target power set to 0.8 and alpha level to 0.05. All data were analyzed with SPSS 24.0 (Chicago, IL) and represented by bar plot with mean and SE (standard error) or box & whisker plot with median and IQR (interquartile range).

SUPPLEMENTARY VIDEO LEGEND

Video S1 – Calcium imaging video.

Representative video recording (30 min) of *ex-vivo* VTA slice (300 µm) of adult (P90) mouse injected with GCaMP6f-AAV. Multiple Ca^{2+}-spiking neurons are visible during ACSF perfusion and after KCl activation. Acquisition rate: 2Hz. Speed: 30x.

SUPPLEMENTARY FIGURES

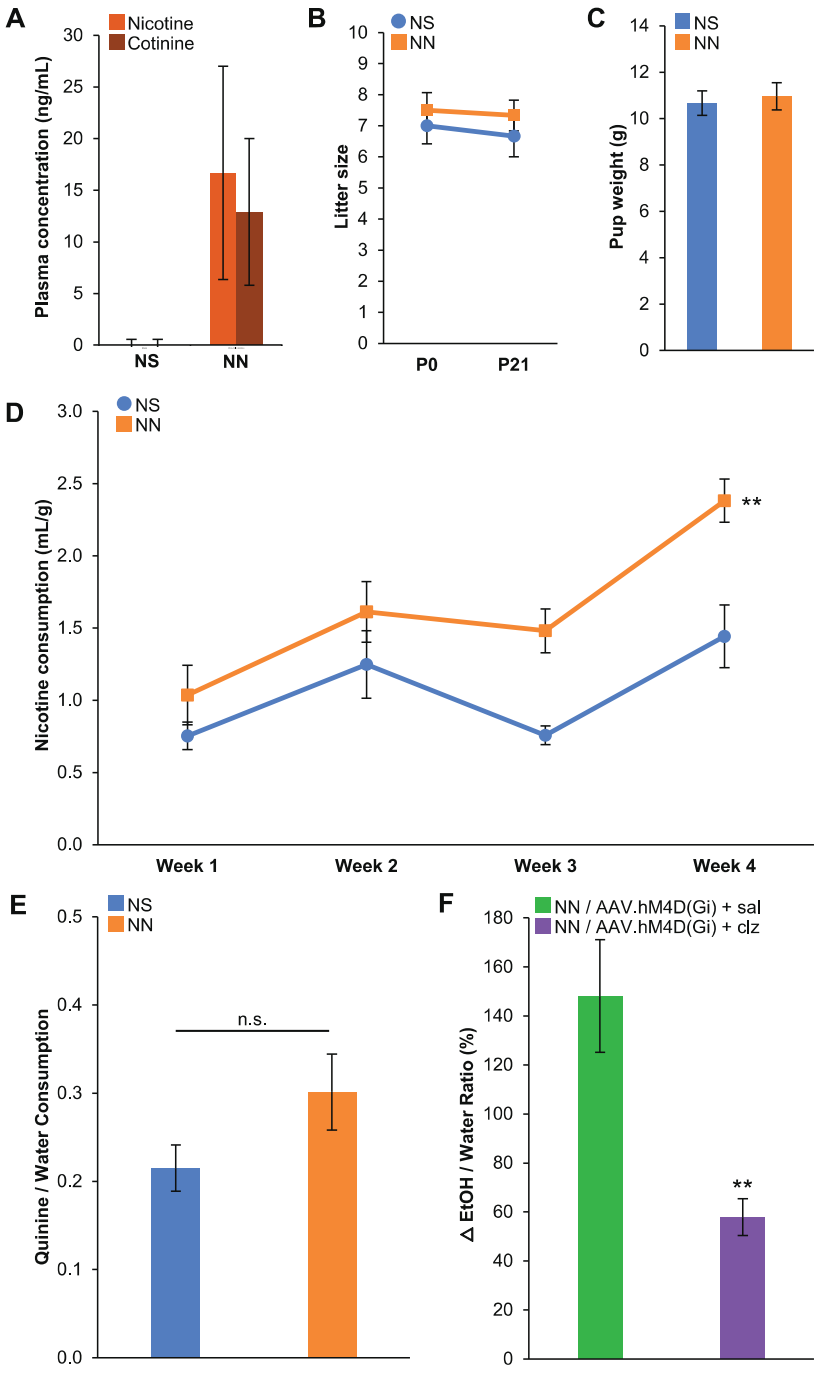

Figure S1 - Neonatal nicotine exposure does not affect litter size or pup weight.

A, NN-exposed pups (P16) show high plasma levels of nicotine and cotinine (N=10 mice per group).

B, NN exposure does not affect pup survival at weaning (P21). N=6 litters per group.

C, NN exposure does not affect pup weight at weaning (N=20 mice per group).

D, Quantification of 75 mg/L nicotine consumption (mL/g) over 4 weeks (N=12 mice/group, Repeated measures ANOVA, NN main effect $F(1,25)=11.54$, $p<0.01$). **$p<0.01$.

E, NN exposure does not affect 2 mM quinine preference (P90, N=6 per group).

F, NN-treated mice no longer display enhanced ethanol preference when VTA neurons are chronically hyperpolarized during the ethanol 2-bottle choice test. (N=6 mice per group, $t(10)=3.74$, $p<0.01$). **$p<0.01$.

All graphs show mean ± SE.

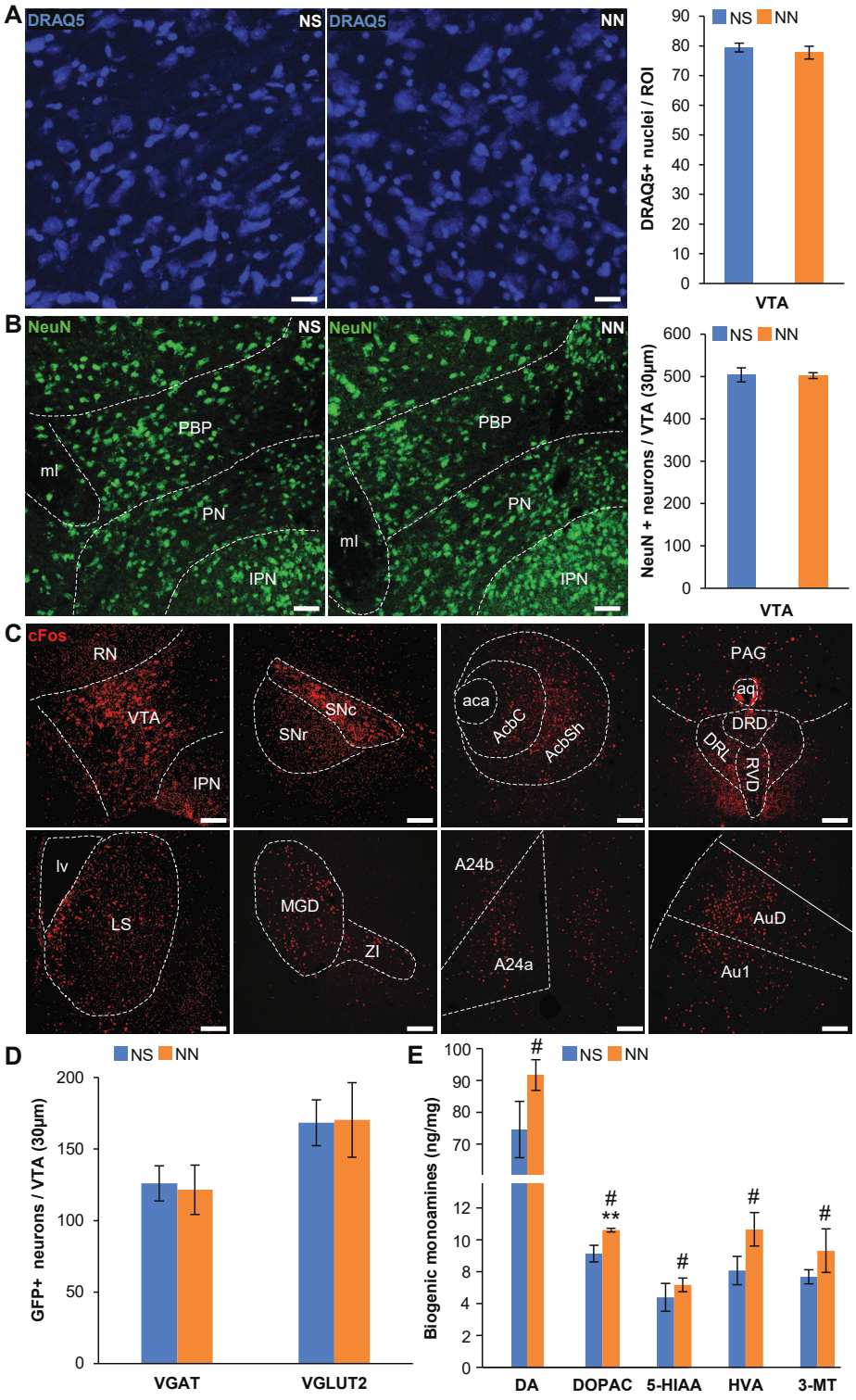

Figure S2 – The total number of cells in the VTA does not change after AN-induced TH induction.

A, Representative confocal images of the VTA showing DRAQ5-labeled cell nuclei in P120 NS- (left) and NN-treated (middle) mice following AN exposure. Epifluorescence quantification (right) shows no difference in nuclear density. Graph shows mean ± SE. N=6 mice per group. Scale bars 50 μm.

B, Representative confocal images of the VTA showing NeuN-labeled neurons in P120 NS- (left) and NN-treated (middle) mice after AN exposure. Epifluorescence quantification (graph) shows no difference in total number of neurons. Graph shows mean ± SE. N=6 mice per group. Scale bars 100 μm. PBP, parabrachial pigmented area; PN, parinigral area; IPN, interpeduncular nucleus; ml, medial lemniscus.

C, Representative confocal images showing cFos IR labeling in NN-treated mice in various brain areas prior AN-exposure (P90). Top (left-to-right panels): VTA, ventral tegmental area; SN, substantia nigra; NAc, nucleus accumbens; DR, dorsal raphe. Bottom (left-to-right panels): LS, lateral septal nucleus; MGD, medial geniculate nucleus; A24, cingulate cortex, Au, auditory cortex. Scale bars: 100 μm.

D, Epifluorescence quantification of GFP-expressing neurons showing no difference in total number of VGAT+ and VGLUT2+ neurons in the VTA of NS- and NN-treated mice following AN-exposure (P120). Graph shows mean ± SE. N=6 mice per group.

E, HPLC quantification of DA and DA metabolites levels in NAc of NS- and NN-treated mice following AN exposure (P120, N=6 mice/group, Multivariate ANOVA #, NN main effect $F(4,1) = 2922$, $p<0.05$, DOPAC pairwise comparison, $p<0.01$). DOPAC, 3,4-Dihidroxyphenilcetic acid; 5-HIAA, 5-Hydroxyindoleacetic acid; HVA, Homovanillic acid; 3-MT, 3-Methoxytyramine. Graph shows mean ± SE. **$p<0.01$.

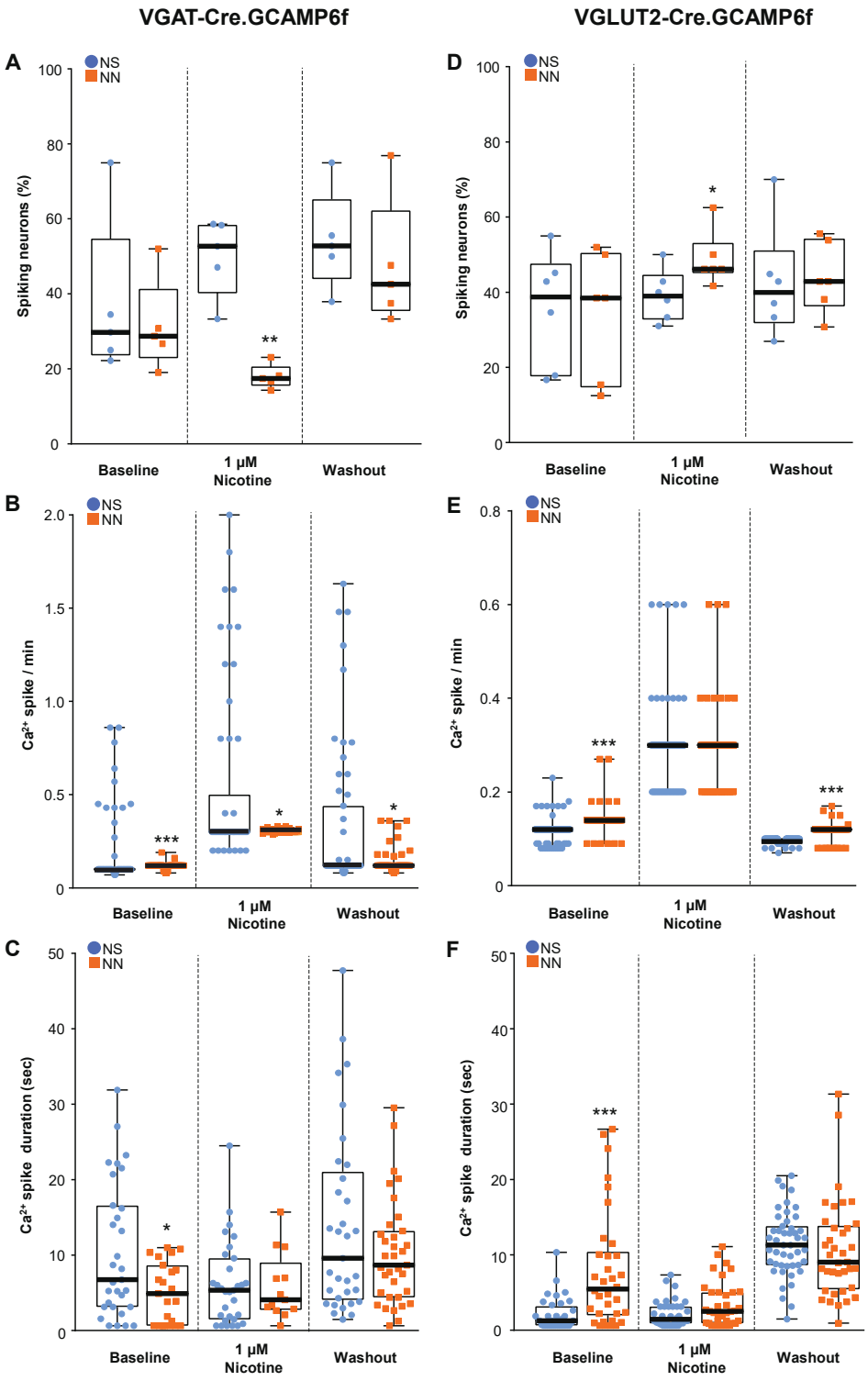

Figure S3 – Neonatal nicotine exposure differentially affects calcium activity in VTA glutamatergic and GABAergic neurons.

A, NN-treated mice display a decrease of active (spiking) GABAergic neurons (%) during 1μM nicotine perfusion (Mann-Whitney U=0, p<0.01, N=5 sections per group).

B, NN-treated mice display enhanced baseline (Mann-Whitney U=1036, p<0.0001), nicotine-evoked (Mann-Whitney U=1380, p<0.05) and washout (Mann-Whitney U=1232, p<0.05) Ca^{2+} spike frequency in VTA GABAergic neurons. N=50 cells per group.

C, NN exposure increases baseline average Ca^{2+} spike duration (Mann-Whitney U=241, p<0.05) in VTA GABAergic neurons. N=30 cells per group.

D, NN-treated mice display an increase of active (spiking) glutamatergic neurons (%) during 1μM nicotine perfusion (Mann-Whitney U=5.5, p<0.05). N=6 sections per group.

E, NN-treated mice display enhanced baseline (Mann-Whitney U=1041, p<0.0001) and washout (Mann-Whitney U=875, p<0.0001) Ca^{2+} spike frequency in VTA glutamatergic neurons. N=70 cells per group.

F, NN exposure increases baseline average Ca^{2+} spike duration (Mann-Whitney U=268.5, p<0.0001) in VTA glutamatergic neurons. N=30 cells per group.

Graphs (a-f) show all data points with medians and IQR. *p<0.05; **p<0.01; ***p<0.001; ****p<0.0001.

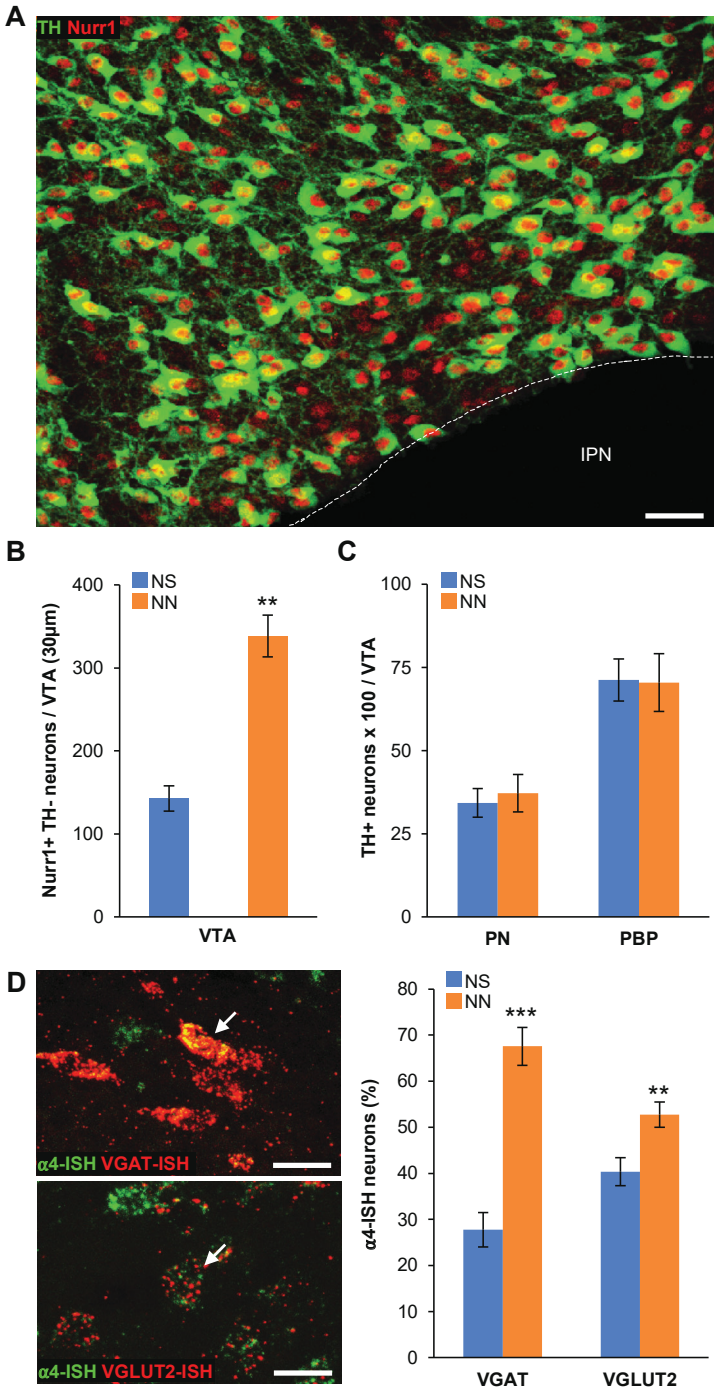

Figure S4 – Neonatal nicotine exposure increases the number of Nurr1+ neurons without affecting TH expression at P16.

A, Representative confocal image of the mouse VTA (P16) immunostained with TH and Nurr1 markers. Scale bar: 50 μm. IPN, Interpeduncular nucleus.

B-C, Epifluorescence quantification shows a significant increase in the number of Nurr1+ TH-negative neurons (b), without affecting TH expression (c) after NN exposure (N=6 mice per group, $t(10)=6.99$, $p<0.01$). Graph shows mean ± SE. **p<0.01.

D, Representative confocal images of α4/VGAT and α4/VGLUT2 double RNAscope in-situ hybridization (left). Quantification (right) shows a significant effect of NN-exposure on the number of VGAT-ISH and VGLUT2-ISH neurons expressing α4-ISH mRNA. (N=8 sections per group, $t(14)=-6.96$, $p<0.001$ VGAT, $t(14)=-3.04$, $p<0.01$ VGLUT2). Graph shows mean ± SE. **p<0.01, ***p<0.001. Scale bar: 20 μm.

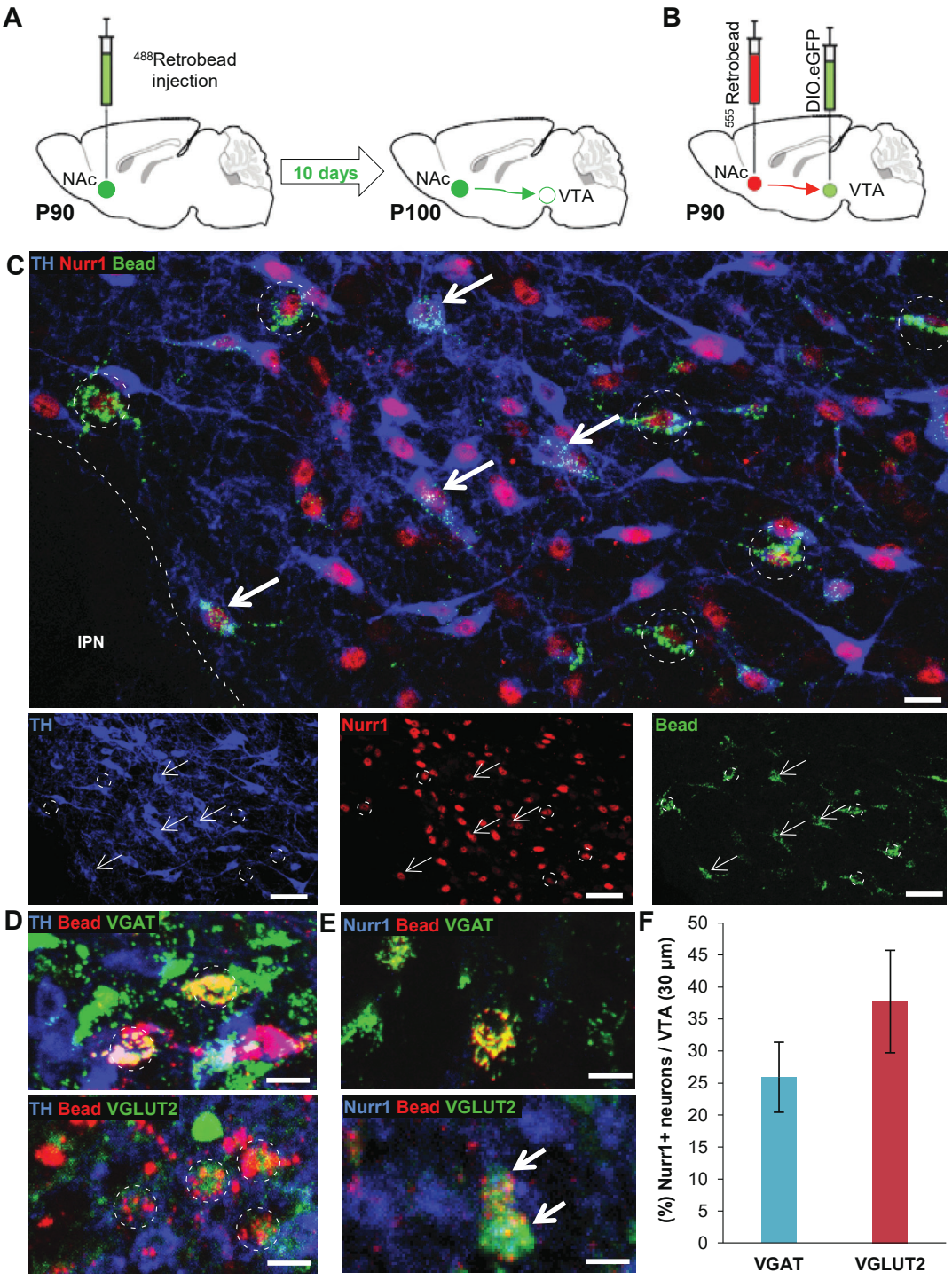

Figure S5 – VTA non-DAergic Nurr1-expressing neurons project to the nucleus accumbens.

A, Schematic diagram showing the site of injection of fluorescent (488 nm) retrobeads (green) in the nucleus accumbens (NAc) of C57BL/6 mice (P90). After 10 days, brain sections were processed for TH and Nurr1 IHC to determine bead localization in the VTA.

B, Schematic diagram showing the site of injection of either retrobeads (555 nm) in the NAc of VGAT-zsGreen mice or concomitant retrobeads in the NAc and AAV.DIO.eGFP in the VTA of VGLUT2-Cre mice, respectively.

C, Representative image of a VTA section immunostained with TH and Nurr1 markers showing both TH-/Nurr1+ (circles) and TH+/Nurr1+ (arrows) VTA-to-NAc projection neurons labeled with retrobeads. Lower panels show the individual channels of the merge image above shown at lower magnification. Scale bars: 20 μm (top); 50 μm (bottom).

D, Representative VTA sections of P90 mice injected as described in (c) processed for TH IHC. Circles indicate GABAergic (top) and glutamatergic (bottom) VTA-to-NAc projection neurons that are TH-negative. Scale bars: 25 μm.

E, Representative VTA sections of P90 mice injected as described in (c) processed for Nurr1 IHC. Arrows indicate Nurr1+ glutamatergic (bottom) VTA-to-NAc projection neurons. Scale bars: 25 μm.

F, Epifluorescence quantification (%) of Nurr1+ NAc-projecting VGAT or VGLUT2 neurons. N=6 sections per group. Graph shows mean ± SE.

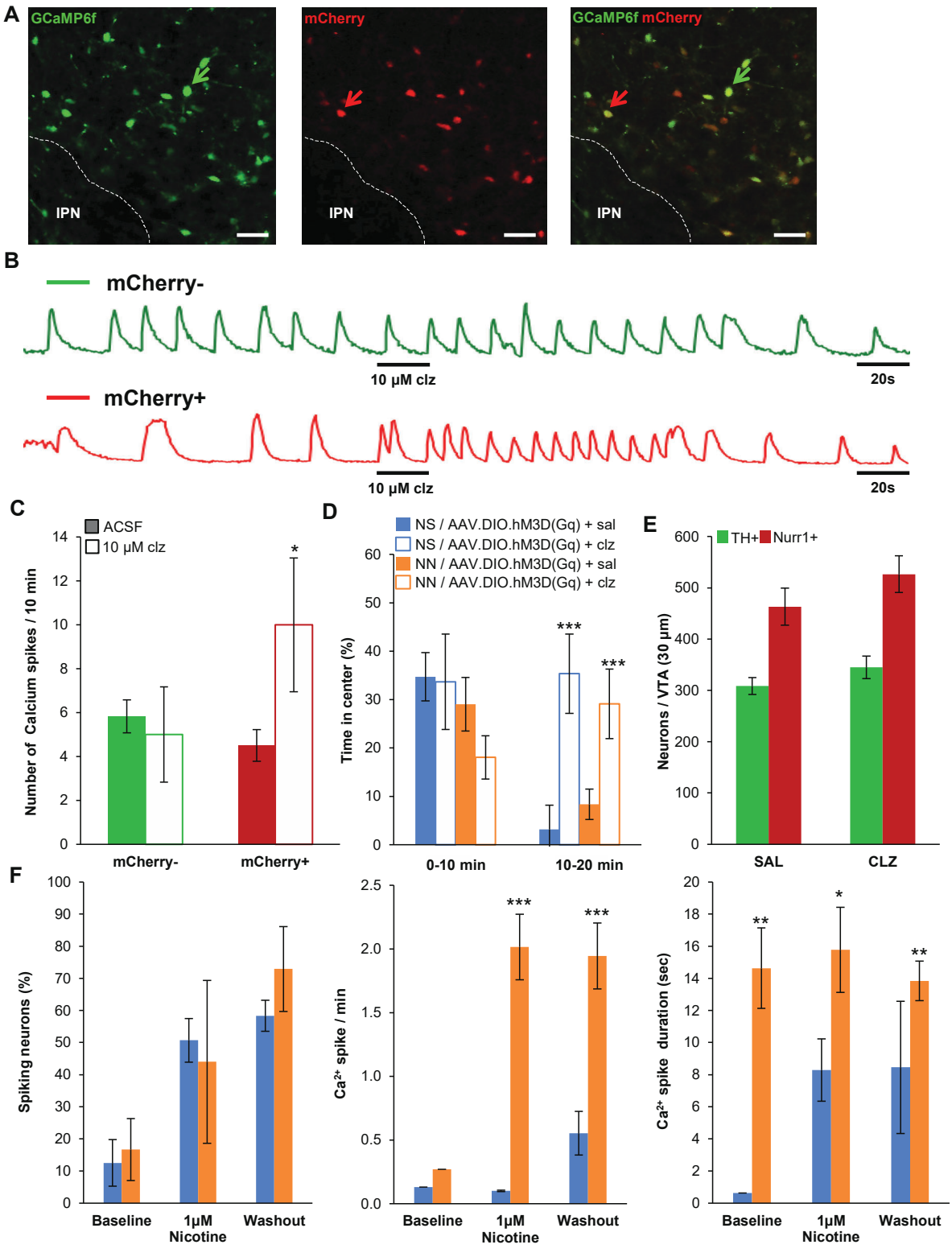

Figure S6 – Validation of DREADD-induced hyperactivation of VTA neurons.

A, Representative confocal images of ex vivo VTA sections showing GCaMP6f and mCherry staining in VGLUT2-Cre mice injected with a mix of AAV.GCaMP6f and AAV.DIO.hM3Dq.mCherry. Arrows indicate representative DREADD+ (mCherry+, red) and DREADD- (mCherry-, green) GCaMP6f-expressing cells. Scale bar: 100 μm.

B, Representative calcium traces recorded from mCherry+ (red arrow in **a**) and mCherry- (green arrow in **a**) neurons before and after slice perfusion with 10 μM clozapine (CLZ).

C, Quantification shows a significant increase in calcium spike frequency induced by CLZ in mCherry+ DREADD-expressing neurons. Graph shows mean ± SE. N=6 mice per group, *p<0.05.

D, Quantification shows VGLUT2-Cre mice injected AAV.DIO.hM3Dq.mCherry spend significantly more time in the center of the OF arena after single IP injection of CLZ at 10 min of the trial (N=8 mice per group, $F(1,27)=18.99$, $p<0.001$). Graph shows means ± SE. ***p<0.001.

E, Epifluorescence quantification shows no effects of chronic CLZ treatment on the number if TH and Nurr1 IR neurons of the VTA. N=6 mice per group. Graph shows mean ± SE.

F, Graph showing the effects of 15 min nicotine (1μM) application on calcium spike. NN-exposed mice show increased calcium spike frequency during (Mann-Whitney U=0, p<0.001) and after (Mann-Whitney U=120.5, p<0.001) nicotine perfusion. NN-treatment increases calcium spike duration across all experimental phases (baseline, Mann-Whitney U=0, p<0.01; nicotine Mann-Whitney U=78, p<0.05; washout Mann-Whitney U=94.5, p<0.01). N=10~20 cells per group. Graphs show mean ± SE.

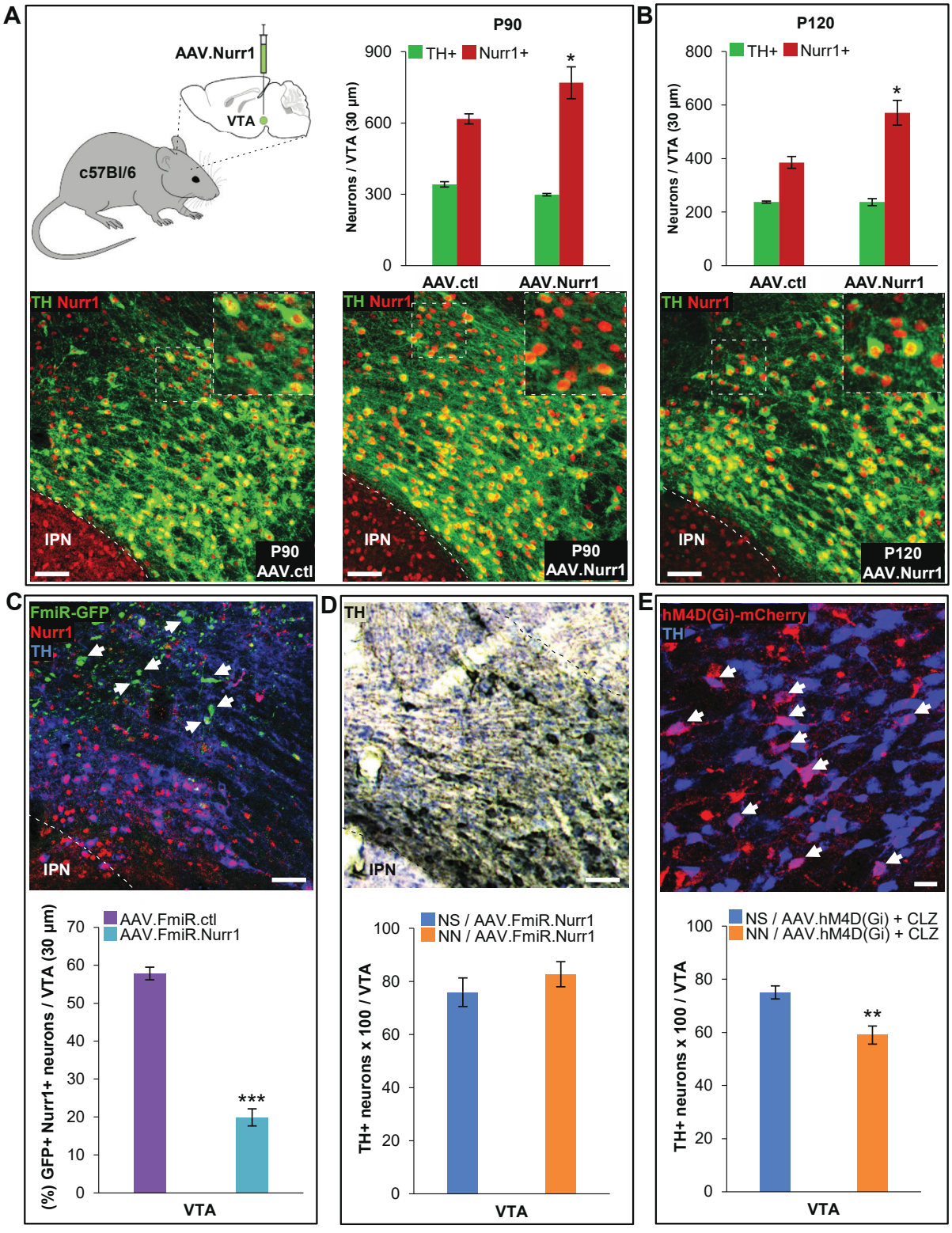

Figure S7 – Validation and effects of Nurr1 and activity manipulation.

A, Adult mice (P70) were injected in the VTA with either a TRMS.Nurr1 AAV or TRMS.ctl AAV vectors. Nurr1 overexpression was evaluated at P90 by IHC with TH and Nurr1 markers (bottom). Insets (dashed box) are shown at higher magnification on the right top corner of each image. Quantification shows a significant increase in the number of Nurr1+ neurons in the VTA of mice P90 (N=6 mice per group, $t(10)=3.03$, $p<0.05$) that does not affect TH expression. Graph shows mean ± SE. *p<0.05. Scale bar: 100 μm.

B, Representative confocal images of the VTA immunostained with Nurr1 and TH markers in mice injected at P70 with either TRMS.ctl AAV or TRMS.Nurr1 AAV vectors then exposed to AN from P90 through P120. DAB stereological quantification performed following AN exposure (P120) shows no changes in the number of TH+ neurons in spite of a significant increase in the number of Nurr1+ neurons in the VTA (N=6 mice per group, $t(10)=-3.62$, $p<0.05$). Graph shows mean ± SE. *p<0.05. Scale bars: 100 μm.

C, Representative image of the VTA showing GFP+ (arrows), Nurr1+, and TH+ neurons in VGLUT2-Cre mice injected with a FmiR.Nurr1 AAV vector. Epifluorescence quantification (%) of GFP+ transfected neurons expressing Nurr1 in the VTA of mice injected with either FmiR.ctl or FmiR.Nurr1 AAV vectors showing a significant Nurr1 downregulation in GFP+ VGLUT2-cre expressing neurons (N=6 sections per group, $t(10)=13.46$, $p<0.001$). ***p<0.001. Graph shows mean ± SE.

D, Representative DAB image of the VTA showing TH IR neurons of mice injected with a FmiR.Nurr1 AAV vector. Stereological quantification of TH IR (DAB) in the VTA of NN/AN-exposed mice (P120) shows that selective Nurr1 downregulation within glutamatergic neurons during AN consumption abolishes the increase in the number of DAergic neurons (N=6 mice per group). Graph shows mean ± SE. Scale bars: 100 μm.

E, Representative VTA section showing TH IR in WT mice injected with hM4D(Gi) AAV. Stereological quantification of the total number of TH+ (DAB) neurons in the VTA shows a decrease in the number of DAergic neurons in NN-exposed mice (P120) treated with CLZ (N=6 mice per group, $p<0.01$). **$p<0.01$. Graph shows mean ± SE. Scale bars: 50 μm.

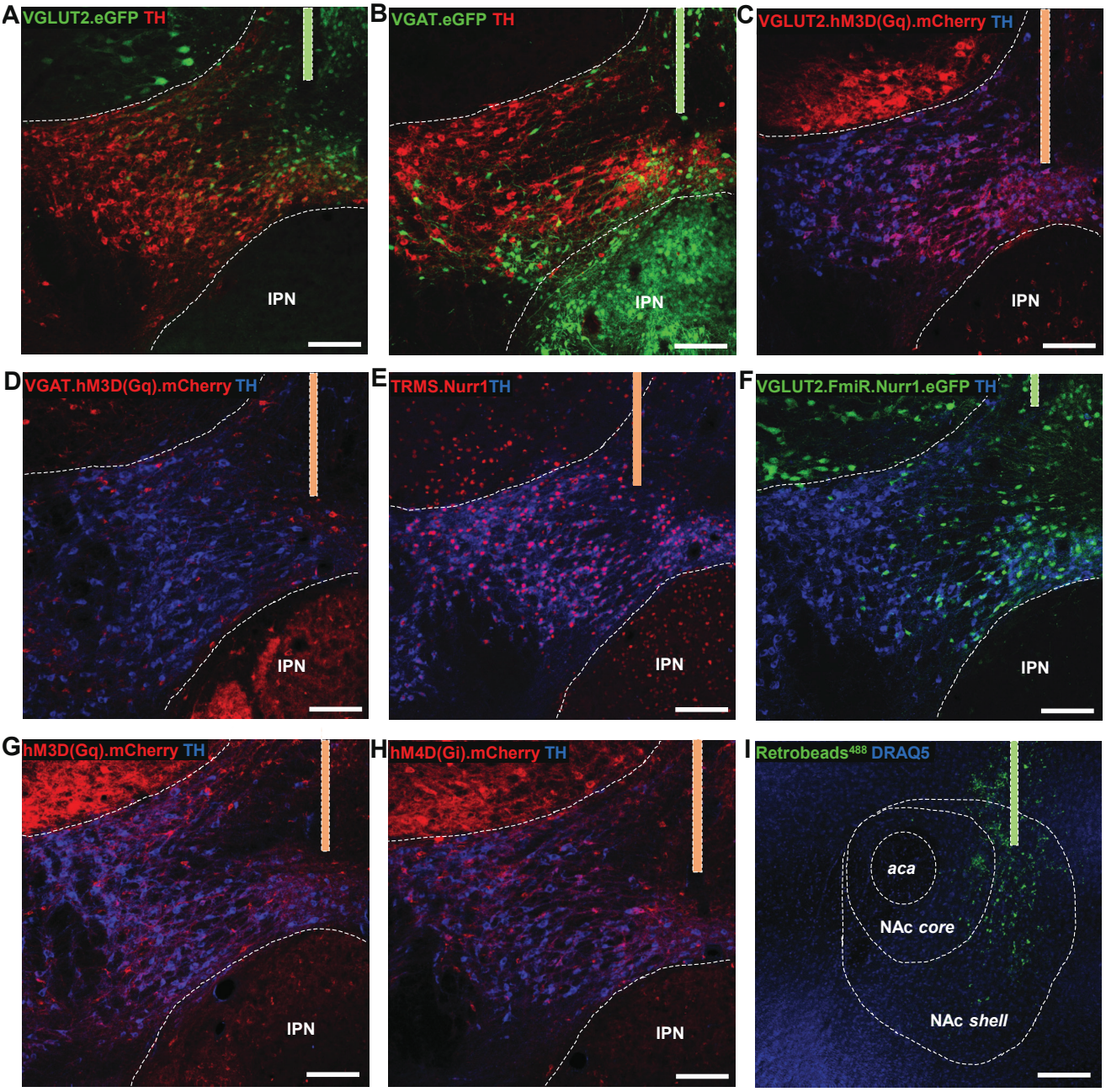

Figure S8– Injection site validation.

Representative low-magnification confocal images showing viral injection sites (dashed bar) for AAV.DIO.eGFP in VGLUT2-Cre (A) and VGAT-Cre (B) mice; AAV.DIO.hM3D(Gq) in VGLUT2-Cre (C) and VGAT-Cre (D) mice; AAV.TRMS.Nurr1 (E);

AAV.FLEX.TRSH.Nurr1 in VGLUT2-Cre mice (F); AAV.hM3D(Gq) (G), AAV.hM4D(Gi) (H); retrobeads in NAc shell (I). Scale bars: 100 µm.

SUPPLEMENTARY TABLE

Table S1 – Calcium imaging summary statistics

Table reporting exact values of mean, median, mode, standard deviation (SD), standard error (SE) and interquartile range (IQR) for graphs in Fig. 3f (top) and 3g (bottom).

Summary Statistics of Fig. 3f (Frequency)						
	baseline		nicotine		washout	
	NS	NN	NS	NN	NS	NN
mean	0.504	0.587	0.464	0.678	0.172	0.499
median	0.140	0.170	0.300	0.350	0.170	0.180
mode	0.140	0.120	0.300	0.300	0.170	0.180
SD	0.632	0.635	0.404	0.596	0.033	0.563
SE	0.053	0.054	0.036	0.052	0.003	0.050
IQR	0.605	0.800	0.000	0.568	0.000	0.370

Summary Statistics of Fig. 3g (Duration)						
	baseline		nicotine		washout	
	NS	NN	NS	NN	NS	NN
mean	10.934	14.351	6.191	13.466	4.226	8.523
median	7.790	11.240	4.770	9.350	2.160	5.815
mode	0.630	2.390	0.630	1.890	0.630	0.630
SD	8.901	11.932	4.854	11.994	4.310	7.549
SE	1.056	1.287	0.649	1.301	0.566	0.909
IQR	12.560	16.640	5.890	13.528	5.590	8.690

SUPPLEMENTARY REFERENCES

1. Dulcis D, Jamshidi P, Leutgeb S, Spitzer NC (2013): Neurotransmitter switching in the adult brain regulates behavior. *Science (80-)*. doi: 10.1126/science.1234152.

2. Chang KT, Berg DK (2001): Voltage-gated channels block nicotinic regulation of CREB phosphorylation and gene expression in neurons. *Neuron*. doi: 10.1016/S0896-6273(01)00516-5.

3. Lippi G, Fernandes CC, Ewell LA, John D, Romoli B, Curia G, *et al.* (2016): MicroRNA-101 Regulates Multiple Developmental Programs to Constrain Excitation in Adult Neural Networks. *Neuron*. doi: 10.1016/j.neuron.2016.11.017.

4. Saunders A, Johnson CA, Sabatini BL (2012): Novel recombinant adeno-associated viruses for Cre activated and inactivated transgene expression in neurons. *Front Neural Circuits*. doi: 10.3389/fncir.2012.00047.

5. Benskey MJ, Sandoval IM, Manfredsson FP (2016): Continuous Collection of Adeno-Associated Virus from Producer Cell Medium Significantly Increases Total Viral Yield. *Hum Gene Ther Methods*. doi: 10.1089/hgtb.2015.117.

6. Ting JT, Daigle TL, Chen Q, Feng G (2014): Acute brain slice methods for adult and aging animals: Application of targeted patch clamp analysis and optogenetics. *Methods Mol Biol*. doi: 10.1007/978-1-4939-1096-0_14.

7. Gomez JL, Bonaventura J, Lesniak W, Mathews WB, Sysa-Shah P, Rodriguez LA, *et al.* (2017): Chemogenetics revealed: DREADD occupancy and activation via converted clozapine. *Science (80-)*. doi: 10.1126/science.aan2475.

8. Meliska CJ, Bartke A, McGlacken G, Jensen RA (1995): Ethanol, nicotine, amphetamine, and aspartame consumption and preferences in C57BL/6 and DBA/2 mice. *Pharmacol Biochem Behav*. doi: 10.1016/0091-3057(94)00354-8.